Dalton Transactions

Large Structural Changes upon Protonation of Fe4S4 Clusters: the Consequences for Reactivity.

Journal:	*Dalton Transactions*
Manuscript ID:	DT-ART-06-2014-001687.R1
Article Type:	Paper
Date Submitted by the Author:	01-Jul-2014
Complete List of Authors:	Dance, Ian; University of New South Wales, Chemistry Henderson, Richard; Newcastle University, Chemistry

Large Structural Changes upon Protonation of Fe_4S_4 Clusters: the Consequences for Reactivity.

Ian Dance[a] and Richard A. Henderson[b]

[a] School of Chemistry, University of New South Wales, Sydney 2052, Australia.

[b] School of Chemistry, Newcastle University, Newcastle upon Tyne, NE1 7RU, UK.

Abstract

Density functional calculations reveal that protonation of a μ_3-S in $[Fe_4S_4X_4]^{2-}$ clusters (X = halide, thiolate, phenoxide) results in the breaking of one S-Fe bond (to > 3Å, from 2.3Å). This creates a doubly-bridging SH ligand (μ_3-SH is not stable), and a unique three-coordinated planar Fe atom. The under-coordination of this unique Fe atom is the basis of revised mechanisms for the acid-catalysed ligand substitution reactions in which substitution of X by PhS occurs at the unique Fe site by an indirect pathway involving initial displacement of X by acetonitrile (solvent), followed by displacement of coordinated acetonitrile by PhSH. When X = Cl or Br the rate of attack by PhSH is slower than the dissociation of X^-, and is the rate-determining step; in contrast, when X = SEt, SBu^t or OPh the rate of dissociation of XH is slower than attack by PhSH and is rate-determining for these clusters. A full and consistent interpretation of all kinetic data is presented including new explanations of many of the kinetic observations on the acid-catalysed substitution reactions of $[Fe_4S_4X_4]^{2-}$ clusters. The proposed mechanisms are supported by density functional calculations of the structures of intermediates, and simulations of some of the steps. These findings are expected to have widespread ramifications for the reaction chemistry of both natural and synthetic clusters with the $\{Fe_4S_4\}$ core.

Introduction

Cubanoid clusters, typified by $\{Fe_4S_4\}^{2+}$, are widespread in biology and are commonly associated with electron transfer reactions. In addition, in enzymes such as carbon monoxide dehydrogenase CODH ($NiFe_4S_5$), aconitase (cubanoid Fe_4S_4) and the Mo-based nitrogenase ($MoFe_7S_9C$ = FeMo-co) the clusters constitute the active sites.[1-7] Since these proteins operate in a protic environment, it is important to establish the protonation chemistry of Fe-S-based clusters and understand how protonation affects the structure and reactivity of these clusters. Studies on a wide range of synthetic Fe-S-based clusters have shown that protonation by relatively weak acids (*e.g.* $NHEt_3^+$) is pervasive. To illustrate a typical effect of protonation, the half-life for the formation of $[Fe_4S_4(SPh)_4]^{2-}$ from $[Fe_4S_4Cl_4]^{2-}$ (0.1 mmol dm^{-3}) by 10 mmol dm^{-3} PhSH is decreased from 350 ms to 5.7 ms in the presence of 20 mmol dm^{-3} Et_3NH^+. Following density functional (DF) investigations of the protonation of μ_3-S in FeMo-co,[8] similar calculations revealed that protonation of μ_3-S in $[Fe_4S_4X_4]^{2-}$ (X = thiolate, halide or phenoxide) is associated with cleavage of a Fe-S bond, disrupting the integrity of the cluster core.[9] It is anticipated that this structural change would have profound effects on the reactivity and mechanisms of substitution reactions of these clusters.

The kinetics and mechanisms of acid-catalysed substitution reactions of Fe-S-based clusters have been studied extensively.[10,11] In this paper we reconsider the previously proposed mechanisms of acid-catalysed substitution in the light of the results from the DF calculations. We focus on the geometric and electronic structures of $[Fe_4S_3(SH)X_4]^-$ and present a new interpretation of the kinetics for the acid-catalysed substitution reactions which is a direct consequence of the structural disruption to the cluster core initiated by protonation. Using DF calculations we have simulated the key steps in this new mechanism: addition of the proton; binding of MeCN (solvent) and dissociation of X and binding of PhSH and displacement of coordinated MeCN. Before presenting the results of calculations we will briefly summarise the kinetic results on the acid-catalysed substitution reactions of the isostructural series $[Fe_4S_4X_4]^{2-}$ and indicate where the mechanisms suggested earlier fall short in explaining aspects of the reactivity of the clusters, reactivity which is readily explained by the revised mechanism.

Background: kinetics of the acid-catalysed substitution reactions

Reactions in which protonation is coupled to a substitution step are commonplace in chemistry (*e.g.* most notably the reactions of free and coordinated organic carbonyl compounds[12,13]) and have been identified in the reactions of essentially all synthetic Fe-S-based clusters. In the first study of such reactions (of $[Fe_4S_4(SBu^t)_4]^{2-}$ with aryl thiols), the aryl thiols functioned as both the nucleophile and the acid.[14] To avoid ambiguities in mechanistic interpretation of the kinetics of reactions performed under these conditions, later studies used mixtures of a weak acids and nucleophile (*e.g.* $NHEt_3^+$ and PhSH), allowing the protonation step to be distinguished from the substitution step.[15,16]

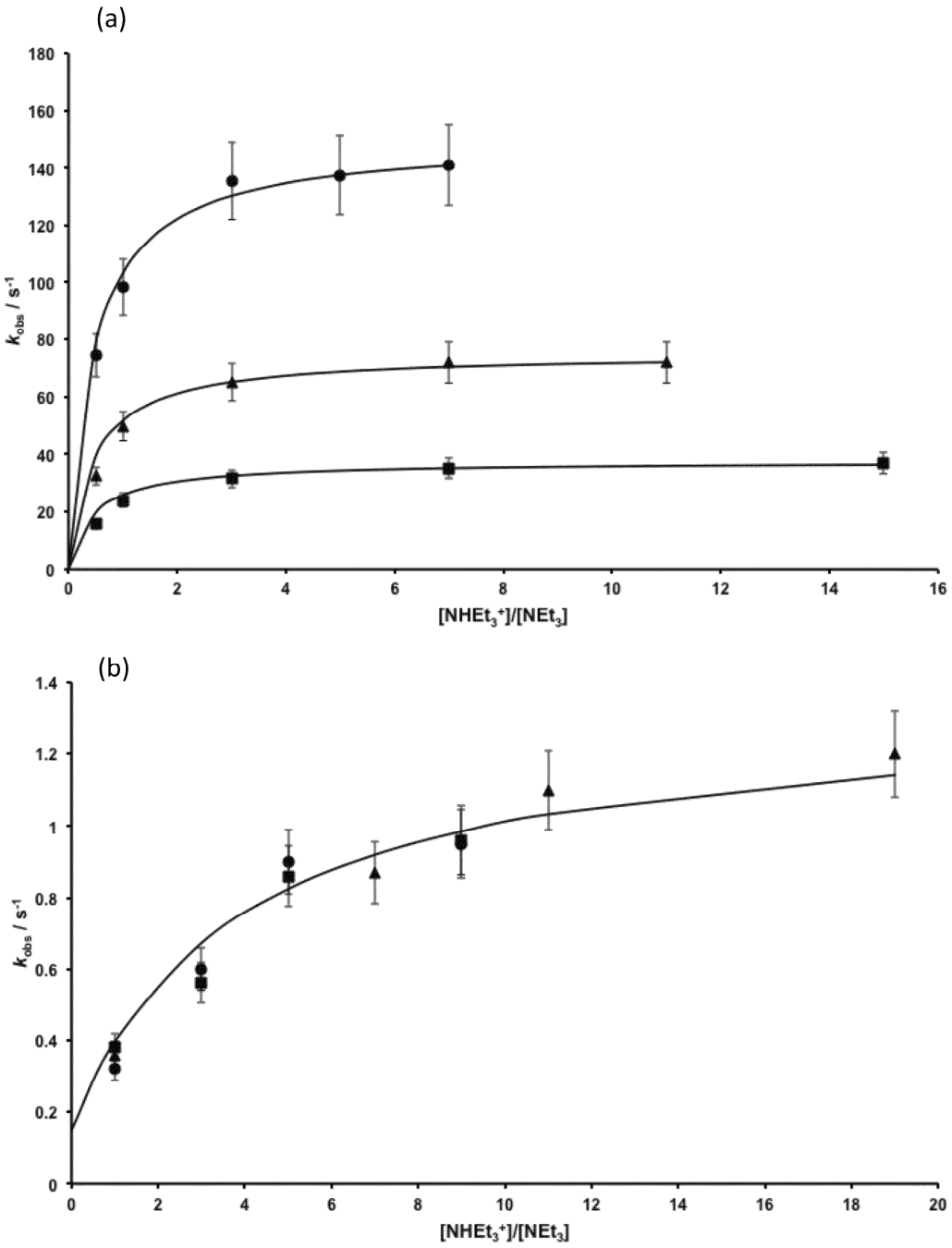

Fig. 1. (a) Dependence of k_{obs} on the ratio $[NHEt_3^+]/[NEt_3]$ for the reaction of $[Fe_4S_4Cl_4]^{2-}$ (0.1 mmol dm^{-3}) with PhSH in MeCN at 25.0 ^oC, showing the dependence of the rate on the concentration of PhSH; [PhSH] = $[NEt_3]$ = 2.5 mmol dm^{-3} (■), [PhSH] = $[NEt_3]$ = 5.0 mmol dm^{-3} (▲), [PhSH] = $[NEt_3]$ = 10.0 mmol dm^{-3} (●). Data is from reference [17]. (b) Dependence of k_{obs} on the ratio $[NHEt_3^+]/[NEt_3]$ for the reaction of $[Fe_4S_4(OPh)_4]^{2-}$ (0.1 mmol dm^{-3}) with PhSH in MeCN at 25.0 ^oC, showing the independence of the rate on the concentration of PhSH; [PhSH] = $[NEt_3]$ = 2.5 mmol dm^{-3} (■), [PhSH] = $[NEt_3]$ = 5.0 mmol dm^{-3} (▲), [PhSH] = $[NEt_3]$ = 10.0 mmol dm^{-3} (●). Under all conditions [PhS-] ≤ 0.01 mmol dm^{-3} and hence [PhSH]/[PhS$^-$] ≥ 250.

The kinetic characteristics of the acid-catalysed substitution reactions of all synthetic Fe-S-based clusters are typified by the results of studies on the series of isostructural cubanoid clusters, $[Fe_4S_4X_4]^{2-}$ (X = SEt,[15] SBu^t,[15] SPh,[15] Cl,[17] Br,[17] and OPh[9]). Comparison of the rates and kinetics of the acid-catalysed substitution reactions of this series of clusters ensures that any differences in reactivity must be attributable to effects of the terminal ligands X (leaving group), and avoids complications associated with changes to reactivity due to differences in the cluster core. With PhSH as nucleophile and $NHEt_3^+$ as the acid, the kinetics for the acid-catalysed substitution reactions of all $[Fe_4S_4X_4]^{2-}$, exhibit a non-linear dependence on $[NHEt_3^+]/[NEt_3]$. The reactions are distinguished by their dependences on the concentration of PhSH. When X = SEt, SBu^t, SPh or OPh, the rate is independent of the concentration of PhSH {as shown for the reaction of $[Fe_4S_4(OPh)_4]^{2-}$ in Fig. 1 (b)}, but when X = Cl or Br, the rate of the reaction exhibits a first order dependence on the concentration of PhSH {as shown in Fig. 1 (a) for the reaction of $[Fe_4S_4Cl_4]^{2-}$}. Previously, we suggested (based only on the dependence of the rate on the concentration of nucleophile) that for X = SEt, SBu^t, SPh or OPh the substitution step follows a dissociative pathway, whilst for X = Cl or Br, the substitution step occurs by an associative mechanism (Fig. 2).[10,11]

As we pointed out recently,[9] although these simple mechanisms rationalise the different dependences on the concentration of nucleophile, there are features that were difficult to reconcile with the mechanisms in Fig. 2. These unexplained features were (1) the slow rates of proton transfer, (2) the absence of a discernable kinetic isotope effect, (3) the apparent pK_a values of the clusters and (4) the fact that protonation facilitates substitution irrespective of the dependence of the rate on the concentration of nucleophile. The recognition, from DF calculations, that protonation of a μ_3-S in $[Fe_4S_4X_4]^{2-}$ involves concomitant Fe-S bond cleavage, leads to a new and comprehensive description of the mechanism of acid-catalysed substitution reactions of Fe-S-based clusters which readily rationalises all experimental observations.

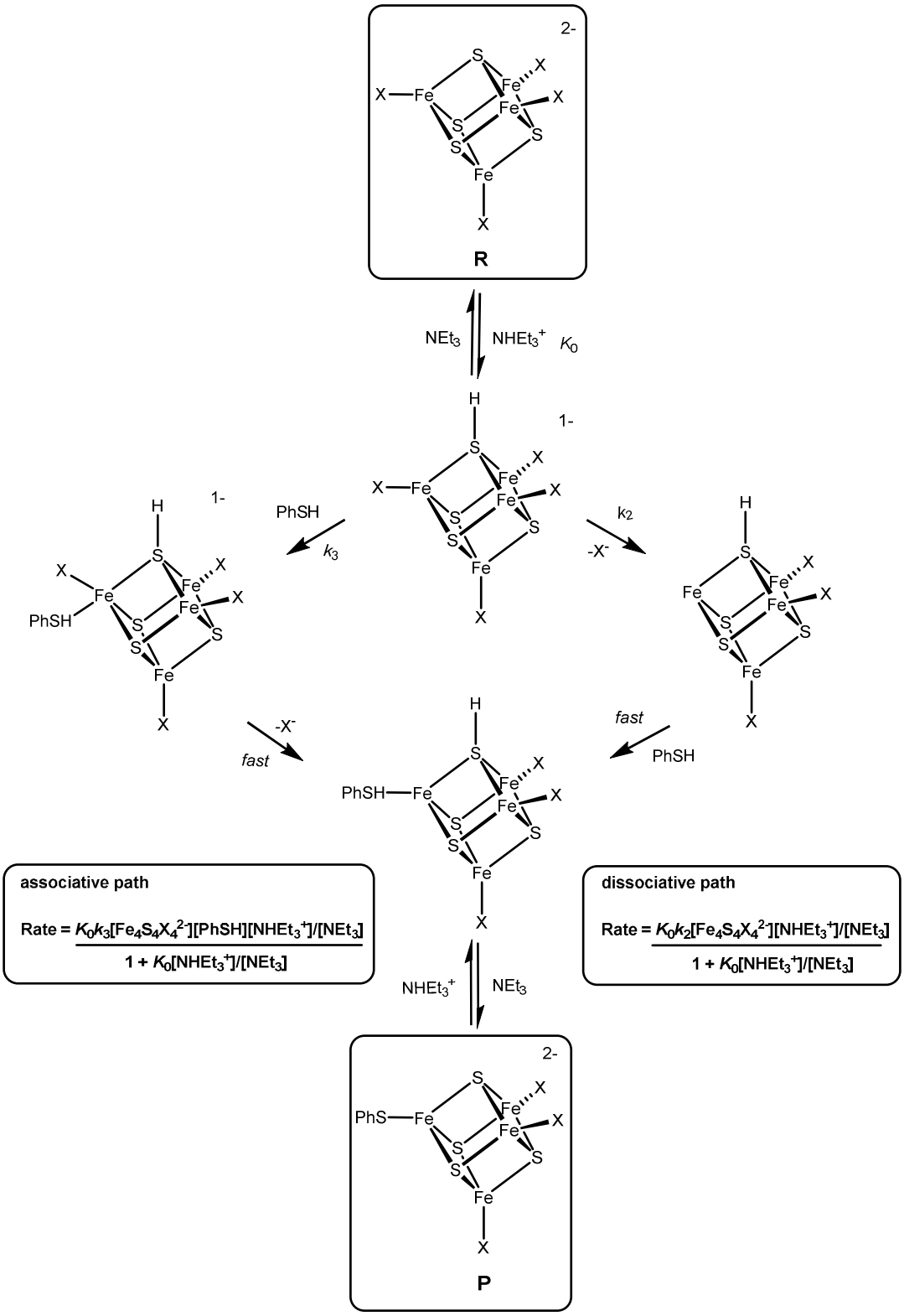

Fig. 2. The previously suggested mechanisms for acid-catalysed substitution reactions of $[Fe_4S_4X_4]^{2-}$, involving associative and dissociative pathways for substitution in which the integrity of the $\{Fe_4S_4\}$ cluster core is retained throughout .

Geometric and electronic structures of $[Fe_4S_3(SH)X_4]^-$

Density functional optimisations of $[Fe_4S_3(SH)X_4]^-$, with representative ligands X = Cl, OMe, OPh, SEt, SPh, reveal elongation of one Fe-S and formation of μ-SH. All calculations reported in this paper use the functional blyp, and numerical basis sets (dnp) as implemented in Delley's DMol3 package.[18-20] The calculations are all-electron, spin unrestricted, with a fine integration mesh. Validation results have been reported.[21-24]] The pyramidal Fe_2(μ-SH) moiety has two possible directions for the SH bond, and therefore two configurational isomers exist for $[Fe_4S_3(SH)X_4]^-$, designated *endo* and *exo*, relative to the elongated S---Fe vector (Scheme 1). In $[Fe_4S_3(SH)X_4]^-$ the elongated Fe^a--SH distance ranges from 2.86 to 3.39Å in the *endo* isomers, and 3.38 to 3.48Å in the *exo* isomers. The two Fe-S(H) bonds forming the μ-SH bridge, ranging 2.39 to 2.48Å, are ca 0.12Å longer than the Fe-S bonds of the original μ_3-S bridge. The stereochemistry of the three-coordinate Fe^a atom (designated the 'unique Fe atom' in the descriptions below) is generally close to planar, and the degree of planarity correlates with the length of the elongated Fe^a--SH distance, as expected. For example, in *exo*-$[Fe_4S_3(SH)(SPh)_4]^-$ the three-coordinate Fe^a is 0.1Å from its coordination plane and the non-ligating SH is 3.38A distant. The ground state structures of all *endo* and *exo* isomers have S=0. The *endo* and *exo* isomers of $[Fe_4S_3(SH)X_4]^-$ are essentially equally stable: the potential energy difference between the isomers is < 1 kcal mol^{-1} for each X. Further details of the ground and excited state structures of $[Fe_4S_3(SH)X_4]^-$ will be published separately, together with theoretical descriptions of the stereochemical course of protonation of $[Fe_4S_4X_4]^{2-}$ according to its electronic state, and information about the mechanism of interconversion of the *endo*- and *exo*-μ-SH isomers.

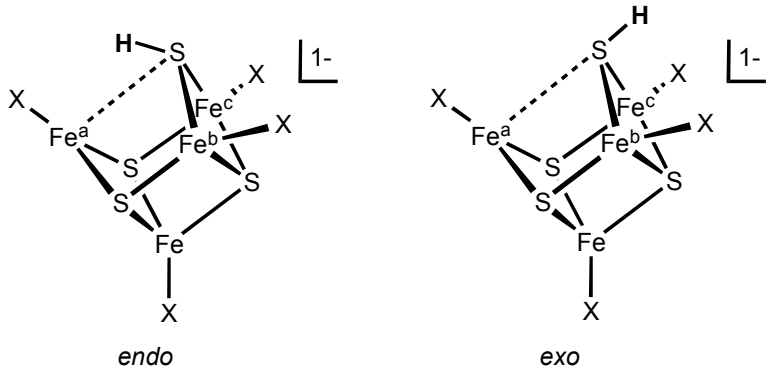

Scheme 1. The *endo* and *exo* isomers of $[Fe_4S_3(SH)X_4]^-$.

When the proton is removed, all forms of $[Fe_4S_3(SH)X_4]^-$ reform the Fe-S bonds without energy barrier and revert to $[Fe_4S_4X_4]^{2-}$.

A new mechanism of acid-catalysed substitution of $[Fe_4S_4X_4]^{2-}$: unifying theory and experiment

Preliminary comments

Probably the most significant feature about these DF results is that they provide a straightforward explanation for the observation that protonation of $[Fe_4S_4X_4]^{2-}$ facilitates substitution irrespective of both the nature of the terminal ligand (X) and the kinetics of the reaction (dependence on the concentration of nucleophile). The major structural change to the cluster core upon protonation is

the origin of this reactivity pattern. The calculations show that cluster disruption following protonation generates an under-coordinated Fe (the unique Fe), a site that is primed for attack by a nucleophile. Thus, after protonation, the labilisation of the terminal ligands to substitution is not a consequence of modified electronic characteristics (caused by adding a positive charge to the cluster), but rather is due to a profound structural modification that facilitates an associative substitution pathway. Consequently, the mechanisms of the substitution of $[Fe_4S_3(SH)X_4]^-$ proposed solely on the kinetics (Fig. 2) need to be reconsidered. In particular, the dissociative pathway suggested for X = SEt, SBu^t, SPh and OPh now seems untenable since a dissociative mechanism would unreasonably involve dissociation of X from the 3-coordinate Fe to generate a 2-coordinate Fe intermediate.

Solution species: acid-base aspects

Central to the discussion of the mechanism of acid-catalysed substitution reactions, is the correlation of experimental rate laws with the calculation results. It is pertinent, therefore, to address here the identities of the solution species (solvent = MeCN), present in the kinetic studies since this relates to the interpretation of the kinetic results. The kinetics of the acid-catalysed substitution reactions of $[Fe_4S_4X_4]^{2-}$ were determined using solutions containing mixtures of $NHEt_3^+$ and PhS^-. In such solutions the protolytic equilibrium shown in Equation (1) is rapidly established. In the presence of an excess of $NHEt_3^+$, the equilibrium lies predominantly to the right hand side ($NHEt_3^+$, pK_a = 18.4;[25] PhSH, pK_a ~21). In a previous study we estimated K_p = 200.[26] Using this value, we typically can calculate that a mixture initially containing $[PhS^-]_0$ = 5 mM and $[NHEt_3^+]_0$ = 10 mM will, at equilibrium, contain $[PhS^-]_{eq}$ = 0.02 mM and $[NHEt_3^+]_{eq}$ = 5.02 mM (*i.e.* $[PhSH]/[PhS^-] = 2.5 \times 10^2$). Thus, in the acid-catalysed substitution reactions the nucleophile is either the predominant PhSH or the very low equilibrium concentrations of PhS^- present. Previously, we have shown for the acid-catalysed substitution of $[Fe_4S_4Cl_4]^{2-}$ that at a constant concentration of PhS^-, the addition of $NHEt_3^+$ results in a decrease in the rate when $[NHEt_3^+] < [PhS^-]$, reaches a minimum when $[NHEt_3^+] = [PhS^-]$, and then the rate increases (in a non-linear fashion) when $[NHEt_3^+] > [PhS^-]$.[17] The decrease in rate when $[NHEt_3^+] < [PhS^-]$, is due to decrease in the concentration of PhS^- {due to the equilibrium in Equation (1)} and the effect this has on the rate of the substitution of $[Fe_4S_4Cl_4]^{2-}$ with PhS^-. This observation indicates that PhSH is a much poorer nucleophile than PhS^- for Fe-S clusters. The increase in rate when $[NHEt_3^+] > [PhS^-]$, is due to protonation of the cluster by the excess of $NHEt_3^+$ to form $[Fe_4S_3(SH)Cl_4]^-$.

$$PhS^- + NHEt_3^+ \underset{}{\overset{K_p}{\rightleftharpoons}} PhSH + NEt_3 \qquad (1)$$

In general, there are two possible sites for protonation of $[Fe_4S_4X_4]^{2-}$: μ_3-S and X. It is important to appreciate a limitation in the kinetic method used to monitor protonation of $[Fe_4S_4X_4]^{2-}$. The rates of acid-catalysed substitution of $[Fe_4S_4X_4]^{2-}$ only provide evidence for protonations which affect the lability of the terminal ligands (X). Consequently, it is possible that whilst protonation at μ_3-S affects the rate of substitution, protonation of coordinated X may not appreciably affect the rate of substitution and therefore be undetectable by the kinetic method. There is no direct experimental information that defines the relative basicities of μ_3-S and the various X of $[Fe_4S_4X_4]^{2-}$. However, the pK_as of some free HX are known in MeCN,[25] and others can be estimated from the pK_as in water.[27] On the basis of the data available for the free HX, the presumed order of basicity of coordinated ligands is OPh > SEt > SPh > μ_3-S >> Cl, Br. Therefore, for the mechanisms of acid

catalysed substitution of $[Fe_4S_4X_4]^{2-}$, when X = Cl it is extremely unlikely that protonation occurs at X (and occurs only at μ_3-S), but when X = OPh, SEt or SPh it is expected that protonation could occur at both X and μ_3-S. Accordingly, different mechanisms are presented below, first for X = OPh, SEt or SPh, and then for X = Cl.

Mechanism for X = OPh, SEt or SPh

The mechanism we propose is shown in Fig. 3, drawn for the case of X = SEt: the intermediates **2** to **7** are shown only with the *exo* conformation of SH, and there is an analogous sequence of intermediates with *endo*-SH, labeled $\mathbf{2^{en}}$ to $\mathbf{7^{en}}$, and energetically indistinguishable from the *exo* isomers. The first step is protonation of ligand X, to form $[Fe_4S_4X_3(XH)]^-$ (**1**). In order to be consistent with the kinetic data, this protonation of X must: (i) occur before further protonation of μ_3-S, and (ii) protonation of **R** to **1** must be predominantly in favour of **1** (equilibrium far to the right hand side). The second step is protonation of μ_3-S (to form **2**) and the creation of the under-coordinated Fe site at which substitution occurs. Note that in **2** there are isomeric possibilities for the topological relationship between the two sites of protonation, EtSH and SH: only the structure **2** drawn in Fig. 3 allows the mechanism to proceed (this point is discussed further below with the theoretical investigations of intermediates). Intermediate **2** is primed for coordination of the nucleophile, MeCN (solvent) at the unique Fe atom (in **3**). After coordination of MeCN, the unique Fe, being now four-coordinate, can dissociate the weak ligand EtSH (intermediate **4**). This dissociation of EtSH is the rate-determining step. The under-coordinated unique Fe atom in (**4**) is primed for attack by the nucleophile PhSH. forming **5**. Once coordinated, PhSH is susceptible to deprotonation (**6**), and the stronger ligand PhS^- then compensates for the dissociation of MeCN to form (**7**). The sequence of reactions is completed when μ-SH is deprotonated and the Fe-(μ_3-S) bond is easily reformed to produce the substituted, intact cuboidal cluster. The final two steps that complete the cycle could occur in the reverse sequence – deprotonation of μ-SH before dissociation of MeCN: the kinetic data does not reveal these latter stages. Deprotonation prior to dissociation of MeCN is an attractive proposal since the reforming of the Fe-(μ_3-S) bond could help drive the dissociation of MeCN through an effective intramolecular nucleophilic attack. However, earlier deprotonation of μ-SH, prior to the final steps, would remove the advantageous reduced coordination of the unique Fe at stage **4**. The retention of μ-SH throughout the sequence is consistent with a greater basicity of μ-S over μ_3-S.

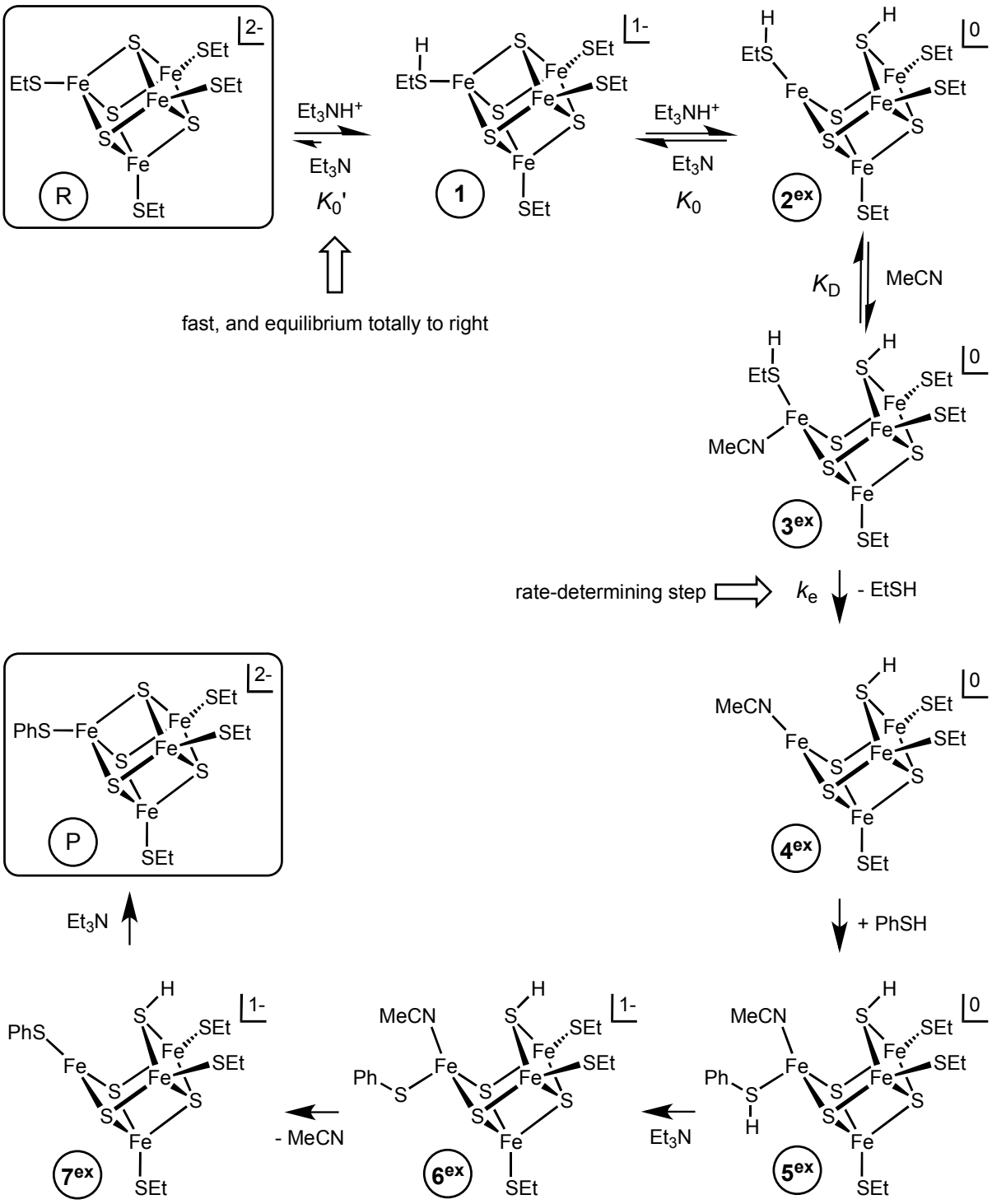

Fig. 3. The mechanism proposed for the substitution of $[Fe_4S_4X_4]^{2-}$ by PhSH, as catalysed by the acid Et_3NH^+, when X = OPh, SEt or SBu^t (illustrated for X = SEt). Intermediates are drawn with the *exo* conformation of SH: an analogous set of intermediates exists for *endo*-SH.

The indirect pathway for substitution of X involving attack of MeCN, rather than direct attack of PhSH on **2**, is dictated by two features. First, the kinetics observed for the reactions involving X = SEt, SBu^t, SPh or OPh where the rate is independent of the concentration of PhSH. Secondly, the formation of the under-coordinated Fe, after protonation, strongly implies an associative

mechanism. Although MeCN may well be a poorer nucleophile than PhSH for Fe-S-based clusters, being solvent it is present in a large excess over the concentration of PhSH ([MeCN]/[PhSH] ~ 2.4 x 10^5). With the dissociation of X = SEt, SBu^t or OPh from **3** as the rate-limiting step in the reaction, the associated rate law is that shown in Equation (2), where $K_D' = K_D[MeCN]$.[28] Values of the elementary rate and equilibrium constants for the mechanism in Fig. 3 are summarised in the ESI.

$$\text{Rate} = \frac{K_0 K_D' k_e [Fe_4S_4X_4^{2-}][NHEt_3^+]/[NEt_3]}{1 + K_0[NHEt_3^+]/[NEt_3]} \qquad (2)$$

The mechanism shown in Fig. 3 assumes that coordinated X is more basic than μ_3-S, and is fully protonated at the outset, and hence the catalysed substitution is of $[Fe_4S_4X_3(XH)]^-$. Because we have no measure of the basicities of the coordinated X, this assumption could be invalid, and, consequently, protonation of μ_3-S is the first step. If so, an alternative mechanism for the early stages of the reactions of the X = SEt, SBu^t or OPh clusters is proposed (Fig. 4). This mechanism is identical to that shown in Fig. 3 except protonation only occurs at a μ_3-S , and the leaving group is X^- rather than XH. The kinetics associated with this mechanism is that presented in Equation (2).

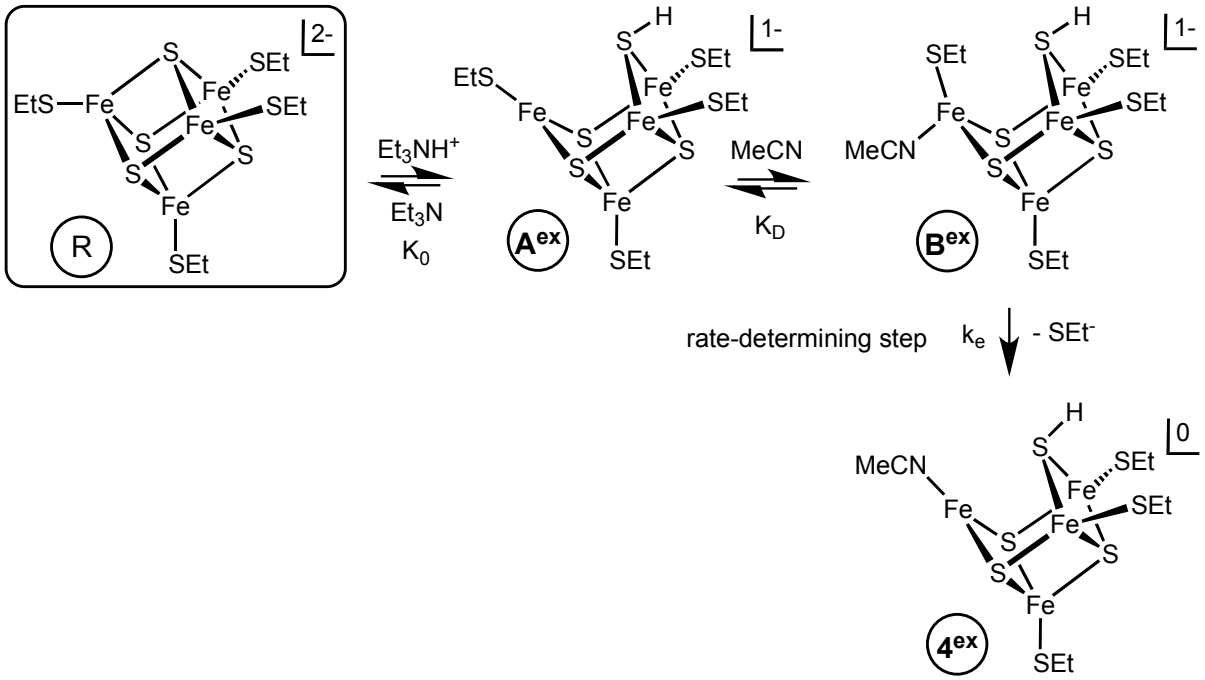

Fig. 4. Alternative early stages of the mechanism for X = SEt, SBu^t or OPh if coordinated X is not protonated. Intermediates **A** and **B** (drawn as *exo* isomers, corresponding *endo* isomers are possible) replace the sequence of intermediates **1**, **2** and **3** of the mechanism in Fig 3. Completion of the mechanism, **4** → **5** → **6** → **7** → **P**, is the same as shown in Fig 3.

Mechanism for X = Cl or Br

This mechanism is shown in Fig. 5. The significant differences from the mechanism in Fig 3 are (a) an absence of initial protonation of Cl in $[Fe_4S_4Cl_4]^{2-}$, because pK_a values indicate this is thermodynamically unfavourable (pK_a^{HCl} = 8.9; pK_a^{NHEt3} = 18.9),[25] (b) fast dissociation of unprotonated Cl^-, and (c) after dissociation of Cl^-, the coordination of PhSH, is the rate-determining step.[29] A feature of the acid-catalysed substitution reactions of the clusters when X = Cl or Br is the marked increase in lability of these ligands compared to the X = Bu^{t}S, EtS, PhS or PhO clusters. This increased lability is also evident in the *uncatalysed* substitution reactions of the parent cluster, $[Fe_4S_4X_4]^{2-}$. For the clusters where X = SPh, SEt, SBu^t or OPh, the kinetics of the uncatalysed substitution are independent of the concentration of nucleophile. The reactions are relatively slow with a half life in the range $t_{1/2}$ = 5 – 116 s.[9,15] For the clusters where X = Cl or Br, the reactions are much faster. The kinetics of the substitution of the X = Cl or Br clusters contains two terms: one is independent of the concentration of nucleophile and the other is dependent on the concentration of nucleophile. For direct comparison with the data for X = SPh, SEt, SBu^t or OPh clusters, the pathways independent of the concentration of nucleophile can only be considered. The reactions of the X = Cl or Br clusters have a half life in the range $t_{1/2}$ = 0.01 – 0.35 s.[17]

We propose that in the reactions with X = Cl or Br clusters the MeCN-assisted displacement of X to form intermediate **Cl-3** also occurs. However, because of the high labilities of X = halide, dissociation of X becomes faster than the displacement of coordinated MeCN by PhSH on **Cl-3**. The rate law associated with the mechanism shown in Fig 5, if the slowest step is attack of PhSH on intermediate **Cl-3**) is that shown in Equation (3).[30] Equation (3) is mathematically of the same form as the experimental rate law for X = Cl or Br shown in Fig. 2, where $K_D' = K_D$[MeCN] and $K_e' = K_e/[Cl^-]$. Values of the elementary rate and equilibrium constants for the mechanism in Fig. 5 are summarised in the ESI.

$$\text{Rate} = \frac{K_0 K_D' K_e' k_f [Fe_4S_4X_4^{2-}][PhSH][NHEt_3^+]/[NEt_3]}{1 + K_0[NHEt_3^+]/[NEt_3]} \qquad (3)$$

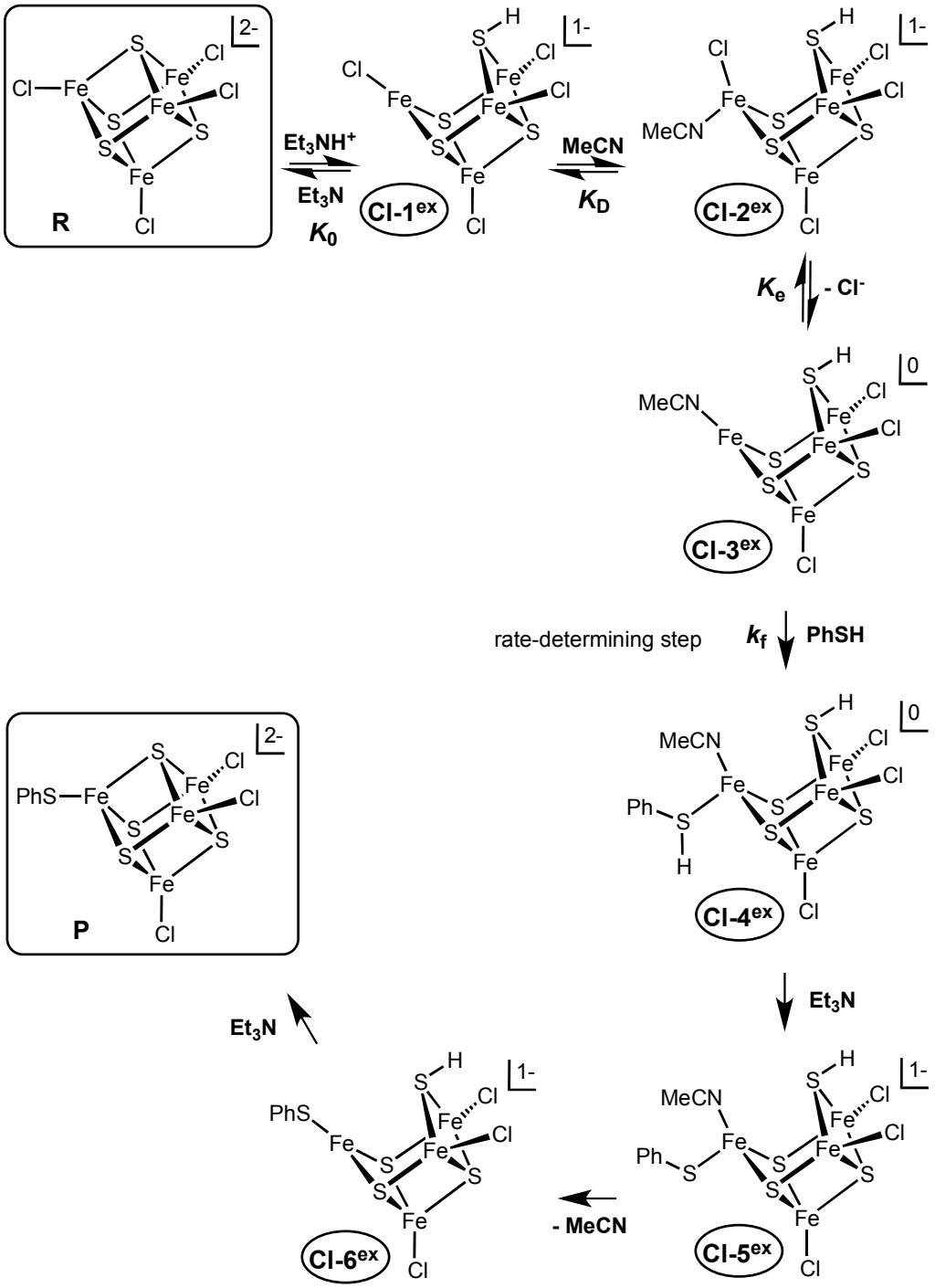

Fig. 5. The mechanism proposed for the substitution of $[Fe_4S_4Cl_4]^{2-}$ by PhSH, as catalysed by the acid Et_3NH^+. Intermediates are drawn with the *exo* conformation of SH: an analogous set of intermediates exists for *endo*-SH.

Density functional simulations of mechanistic details

The intermediates and some of the steps in the mechanisms shown in Figs. 3 and 5 have been investigated by density functional methods. Electronic consistency was maintained through the course of the mechanisms: all species have S=0, and all have the same set of signs for the spin

densities on the four Fe atoms, with oppositely signed Fe spin densities across the μ-SH bridge. Simulations have been made with and without the COSMO model[31-33] of solvation by bulk MeCN (dielectric constant 36). In general the inclusion of solvation effects in this way has minor influence on properties of the intermediates, but in cases of weaker intermolecular interactions the inclusion of COSMO energies has a binding influence. Results with COSMO included are identified as such. Reported energies are potential energies only: thermodynamic corrections are not included. Transition states were located and checked using the method previously developed for the complex trajectories of reactions of the FeMo-co cluster in nitrogenase.[34,35] Pictures and Cartesian coordinates for all intermediates and transition states are provided in the ESI.

The first protonations.

The proton transfer steps, involving Et_3NH^+ and Et_3N, have not been accurately simulated, because the methodology used here is inadequate in describing intermolecular processes in solution. Density functional molecular dynamics, as in the Car-Parrinello method,[36] would be needed to provide a sufficiently accurate representation of the protonation steps in solution.

Protonation of X, intermediate 1, $[Fe_4S_4X_3(XH)]^-$.

In $[Fe_4S_4(SEt)_3(HSEt)]^-$ the Fe-S(H)Et distance is 0.20Å longer than Fe-SEt, and in $[Fe_4S_4(OPh)_3(HOPh)]^-$ the Fe-O distance is increased by 0.38Å on protonation of O. These bond extensions reflect the weaker ligation by and increased lability of the uncharged (protonated) ligands. A requirement of the mechanism for X = SEt, SBu^t or OPh (Fig 3) is that, to be associated with the rate law shown in Equation (2), this protonation of coordinated X must be relatively fast (complete within dead-time of stopped-flow apparatus, 2 ms), and the small geometrical changes, occurring only in the Fe-S(H)Et or Fe-O(H)Ph distances are consistent with this.

Protonation of μ_3-S

Approximate calculations of the transfer of a proton from Et_3NH^+ to μ_3-S of $[Fe_4S_4X_4]^{2-}$ (using COSMO simulation of solvation but no molecular dynamics) have revealed no local energy minima between reactant $\{Et_3NH^+ + [Fe_4S_4X_4]^{2-}\}$ and product $\{Et_3N + [Fe_4S_3(SH)X_4]^-\}$: the proton transfer to S and the Fe--SH elongation processes constitute a single step, with no detectable intermediate.

Prior to these calculations the initial step was assumed to be the simple addition of a proton to μ_3-S of $[Fe_4S_4X_4]^{2-}$ as shown in Fig. 2. Analysis of the kinetics (in particular the non-linear dependence on $[NHEt_3^+]/[NEt_3]$) allowed calculation of the equilibrium constant (K_0) for the initial protonation step.[10,11] Using the value of K_0 and the pK_a of $NHEt_3^+$, the pK_a of the protonated cluster was calculated. It is now evident that the pK_as calculated for the synthetic clusters are not valid since, by definition, a pK_a is a simple acid dissociation constant, but the process with $[Fe_4S_4X_4]^{2-}$ involves both a protonation and a bond cleavage.

The result that protonation of $[Fe_4S_4X_4]^{2-}$ is coupled to Fe-S bond cleavage is fundamental to our interpretation of the experimental parameters associated with proton transfer . The rate of proton transfer from $NHEt_3^+$ to $[Fe_4S_4Cl_4]^{2-}$ (thermodynamically-favoured proton transfer) has been estimated to be $k \leq 1 \times 10^7$ dm^3 mol^{-1} s^{-1},[37] significantly slower than the diffusion-controlled limit ($k = 3.7 \times 10^{10}$ dm^3 mol^{-1} s^{-1} in MeCN).[38] Direct measurement of the rates of proton transfer to the same cluster have been made using pyrrolidinium ion (thermodynamically-unfavourable proton transfer) and $k = 2.4 \times 10^4$ dm^3 mol^{-1} s^{-1}.[39-42] The reverse reaction is thermodynamically-favourable

and can be calculated to be $k \sim 1 \times 10^7$ dm^3 mol^{-1} s^{-1}, confirming the slowness of proton transfer reactions involving $[Fe_4S_4X_4]^{2-}$. It seemed likely that the reason for this slow protonation was because the proton transfer step was associated with significant structural reorganisation of the cluster core dimensions. However, it is only as a consequence of the calculations that it became clear that the barrier for protonation contains contributions from transferring the proton from $NHEt_3^+$ to μ_3-S, and cleavage of the Fe-(μ_3-SH) bond. If this bond breaking constitutes a significant contribution to the overall energy barrier then protonation will be slowed below that expected for simple proton transfer. A further feature of the protonation of $[Fe_4S_4X_4]^{2-}$ is the absence of a measurable kinetic isotope effect associated with this process using deuterated acids.[39] This would be difficult to understand if protonation simply involved the transfer of a proton to the cluster. However, the DF calculations indicate that proton transfer and Fe-(μ_3-SH) cleavage are synchronous. Consequently, the barrier to protonation is a fusion of the barriers to transferring the proton and breaking the Fe-(μ_3-SH) bond. It would be anticipated that the act of proton transfer would be associated with a kinetic isotope effect but the Fe-(μ_3-SH) cleavage would not.

The intermediates **Cl-1^{ex}**, **Cl-1^{en}** (Fig. 5) and **A^{ex}**, **A^{en}** (Fig. 4) have the μ-SH geometries already intimated: the Fe--S(H) distances for the *exo*, *endo* isomers are respectively 3.41, 2.86Å (X = Cl), 3.48, 2.95Å (X = SEt), 3.38, 2.86Å (X = SPh), 3.42, 3.62Å (X = OPh).

Protonation of X and μ_3-S, intermediate 2.

In the mechanism shown in Fig. 3 there is protonation first at X, then at μ_3-S. This introduces the possibility of geometrical isomerism relating to the locations of the two protonation sites, as in Fig. 6. The isomers can be understood in terms of the number of Fe-S bonds separating the protonation sites. The isomer required for the mechanism of Fig. 3 is **2^{ex}** (or **2^{en}**) in which no Fe-S bonds separate the protonation sites, and the protonated X occurs on the unique Fe that has broken its connection to SH. Isomers **2a** have one normal Fe-S bond separating the protonation sites, while in isomers **2b** the protonation sites are as distant as possible, and separated by three intact Fe-S bonds.

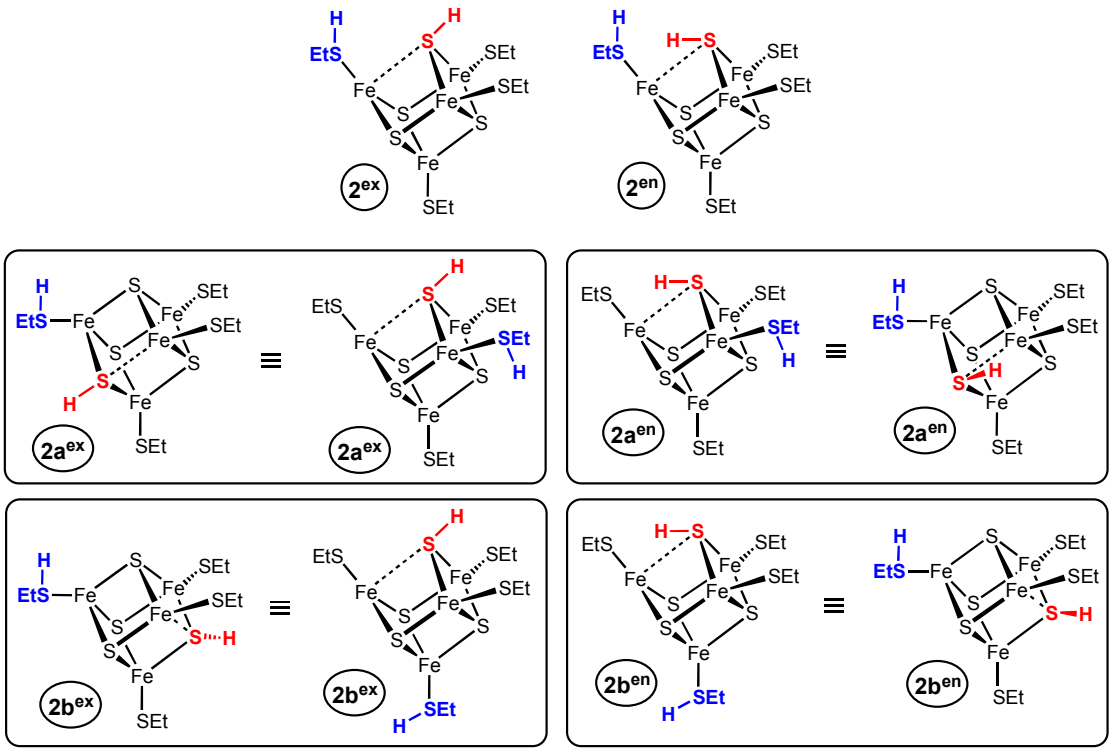

Fig. 6. The six isomers possible for $[Fe_4S_3(SH)X_3(XH)]^0$, drawn for X = SEt. Isomers **2a** have one Fe-S bond separating the protonation sites, while isomers **2b** have a three Fe-S bond separation. Isomers **2a** and **2b** are drawn in two orientations, to facilitate comparisons.

Optimisations of these isomeric possibilities, for X = SEt and X = OPh, reveal that isomers **2a** and **2b** are both slightly more stable than isomers **2**, by 4 - 5 kcal mol^{-1}. Evidently coordination of the more weakly coordinating XH ligand to a four-coordinate Fe is slightly more stable than coordination to the three-coordinate Fe. However, only the isomers **2** with XH bound to the unique Fe have the geometry required to continue the mechanism proposed in Fig 3. For isomers **2a** and **2b** the subsequent dissociation of XH and attack by PhSH would occur at Fe atoms that are similar to those of the uncatalysed reaction, and would not directly benefit from the creation of the unique Fe atom.

Association of solvent MeCN to attain four coordination at the unique Fe atom

As expected, binding of MeCN to the unique Fe on the side remote from the μ-SH is calculated to be a very low energy process, as illustrated in Fig. 7 for the addition of MeCN to $\mathbf{2^{ex}}$ to form $\mathbf{3^{ex}}$, and for conversion of $\mathbf{A^{en}}$ to $\mathbf{B^{en}}$. In both cases the barrier is only 2 kcal mol^{-1}, the transition state occurs when MeCN is far (3.4, 3.1Å) from the three-coordinate Fe atom, and the completion of the MeCN coordination is exergonic (by 13, 8 kcal mol^{-1}).

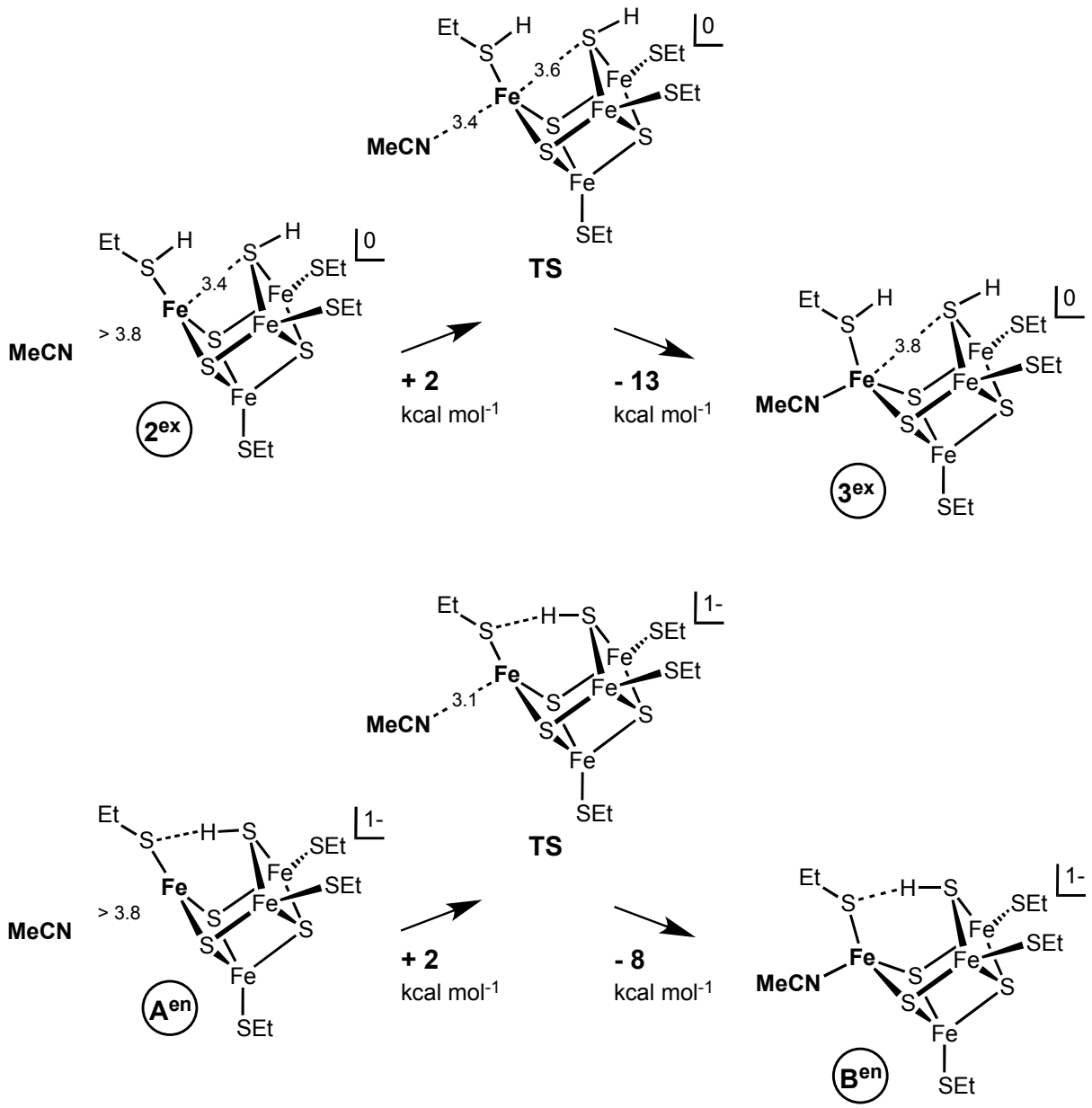

Fig. 7. Two examples of the reaction profile for addition of solvent MeCN to the three-coordinate Fe atom (COSMO energies included). Selected MeCN-Fe and Fe-S interatomic distances (Å) are marked.

The structures of the resulting intermediates are unremarkable. When X = SEt, SBu^t or OPh there are three possible isomers for intermediate **3**, resulting from the possibilities for hydrogen bonds involving the XH or SH functions (see Scheme 2). These hydrogen bonds have minimal stabilising influence: when X = SEt the energy differences between the three isomers are <1.5 kcal mol^{-1} (COSMO energies included). When X = Cl or Br (intermediate **Cl-2^{ex}**, Fig. 5), or in intermediate **B^{ex}** of the alternative mechanism (Fig. 4), the only possible hydrogen bond is from SH.

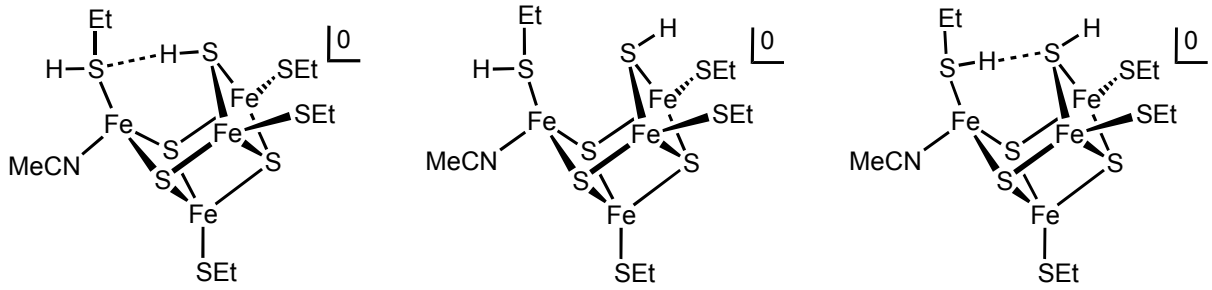

Scheme 2.

Dissociation of XH or X$^-$

When X = Cl or Br, the dissociation is of X$^-$, and is required to be relatively fast in the mechanism shown in Fig. 5 (**Cl-2 → Cl-3)**. Our theoretical methodology does not yield sufficiently accurate simulations of the dissociation of charged ligands X$^-$ (Cl$^-$ or Br$^-$ in the mechanism of Fig. 5, or RS$^-$ or RO$^-$ in the alternative mechanism of Fig. 4).

When X = SEt, SBu^t or OPh the dissociation of XH is the rate limiting step (**3** → **4**) in the mechanism shown in Fig. 3. Energy profiles have been calculated for dissociation of EtSH from the **3^{en}**, **3^{ex}** and **3^{ex-hb}** isomers (Scheme 2) and are represented in Fig. 8. In all cases the potential energy barrier for dissociation of EtSH ranges from 7.7 to 9.3 kcal mol^{-1}, and inclusion of the COSMO solvation energies has only a minor effect. At the transition states, the Fe--S(H)Et distance is very long (ca 4Å), and even though EtSH could be regarded as a weak ligand, these calculations indicate that it needs to stretch a considerable distance from the unique Fe atom in order to dissociate. Note that the dissociation energy barriers and geometries are hardly affected by the absence or presence of different hydrogen bonds involving EtSH. The overall potential energy changes calculated here for dissociation of EtSH (ca 5 to 6 kcal mol^{-1}) are similar to the measured enthalpy of association of EtSH to a five-coordinate ruthenium complex, 5.2 ± 1 kcal mol^{-1}.[43]

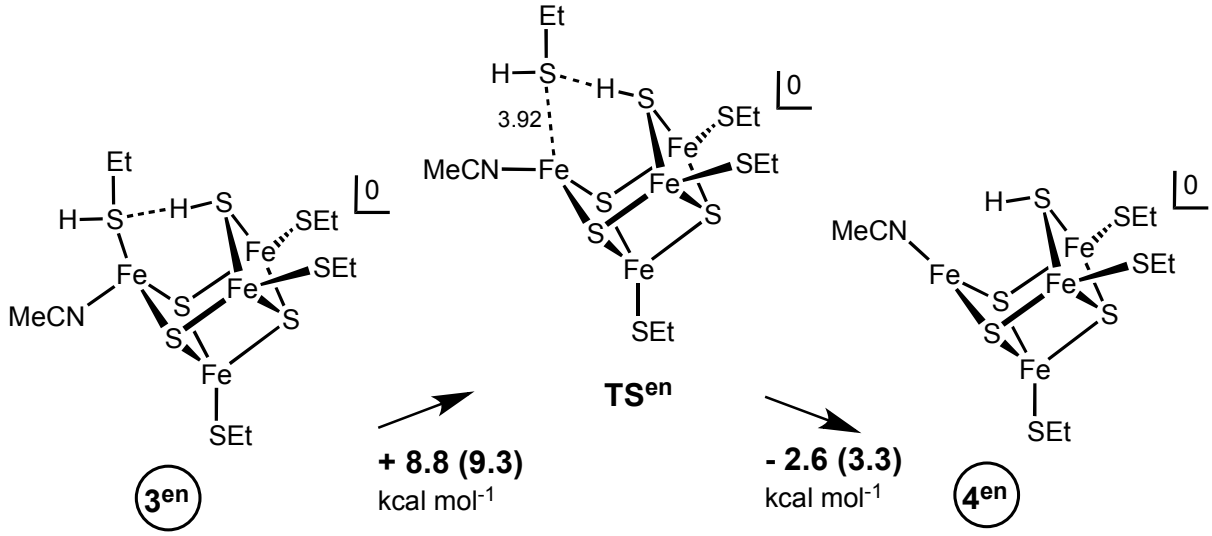

(a)

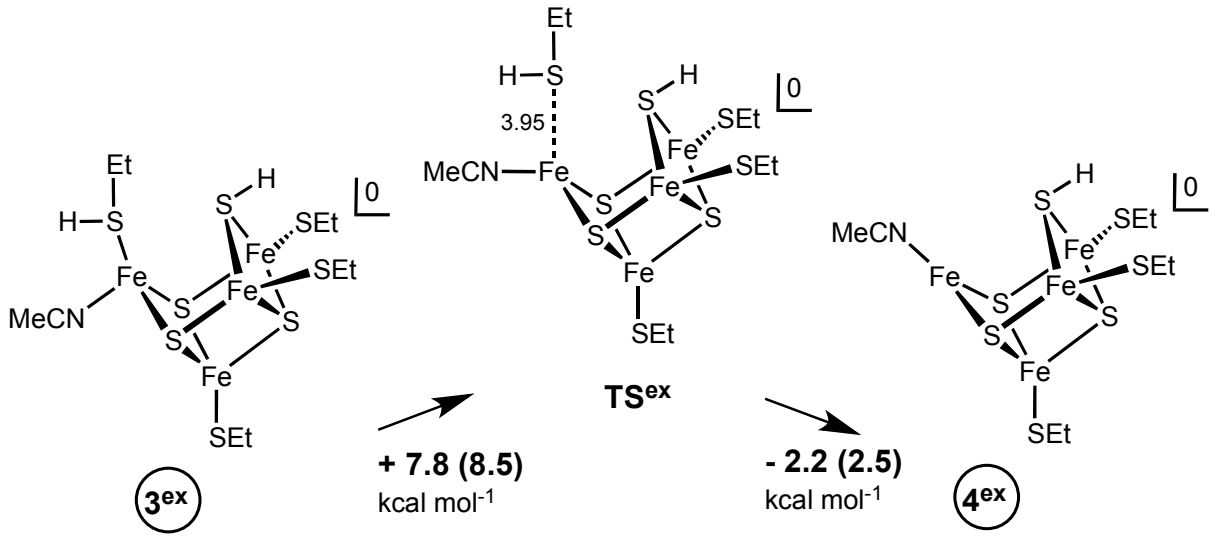

(b)

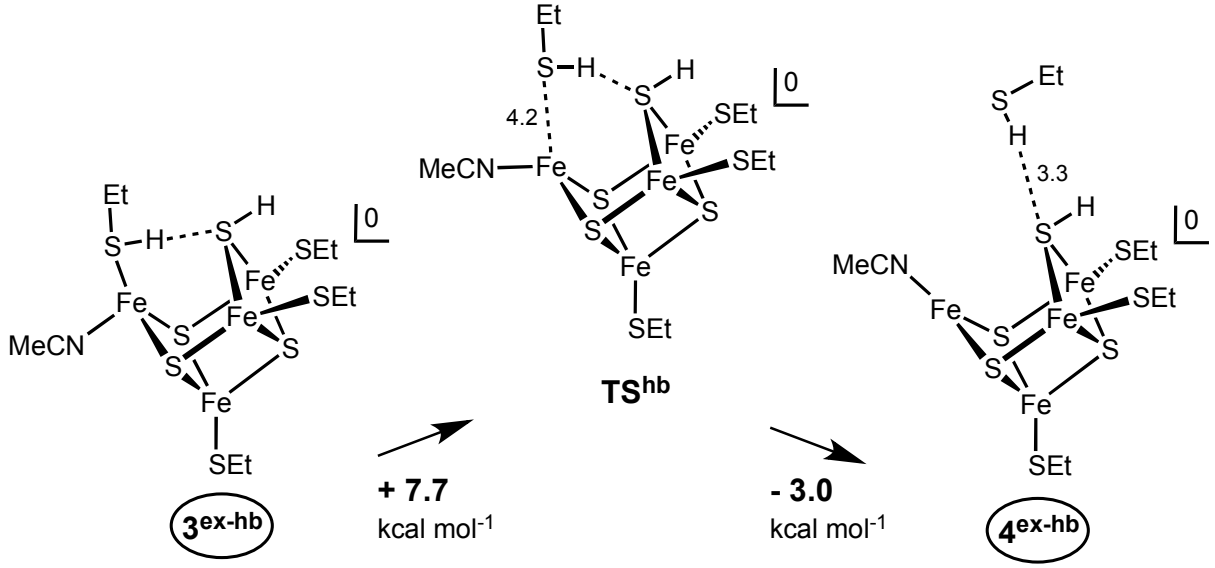

(c)

Fig. 8. Reaction energy profiles for dissociation of EtSH from (a) **3**$^{\mathbf{en}}$, (b) **3**$^{\mathbf{ex}}$ and (c) **3**$^{\mathbf{ex\text{-}hb}}$. Energies with COSMO solvation contributions included are in parentheses. Selected interatomic distances are marked in Å.

Association of PhSH.

The next step (**4** → **5** in Fig. 3, **Cl-3** → **Cl-4** in Fig. 5) involves binding of PhSH to the three-coordinate Fe atom, prior to the dissociation of coordinated MeCN. For X = SEt the four isomers shown in Scheme 3 have been optimised: one conformation of bound PhSH can form a hydrogen bond to a neighbouring SEt ligand, with H--S in the range 2.5 - 2.8Å. Simulations for X = SEt show the binding of PhSH to be both exergonic and barrierless. When PhSH is 3.8Å distant from the under-coordinated Fe atom it undergoes a 8.5 kcal mol^{-1} downhill trajectory to intermediate **5**$^{\mathbf{en\text{-}hb}}$ with a final Fe-S(H)Ph distance of 2.54Å. The corresponding process with incoming PhSH

conformed such that the PhS-H--SEt hydrogen bond cannot form (yielding intermediate **5**^{en}), is calculated to be 6.5 kcal mol^{-1} exergonic.

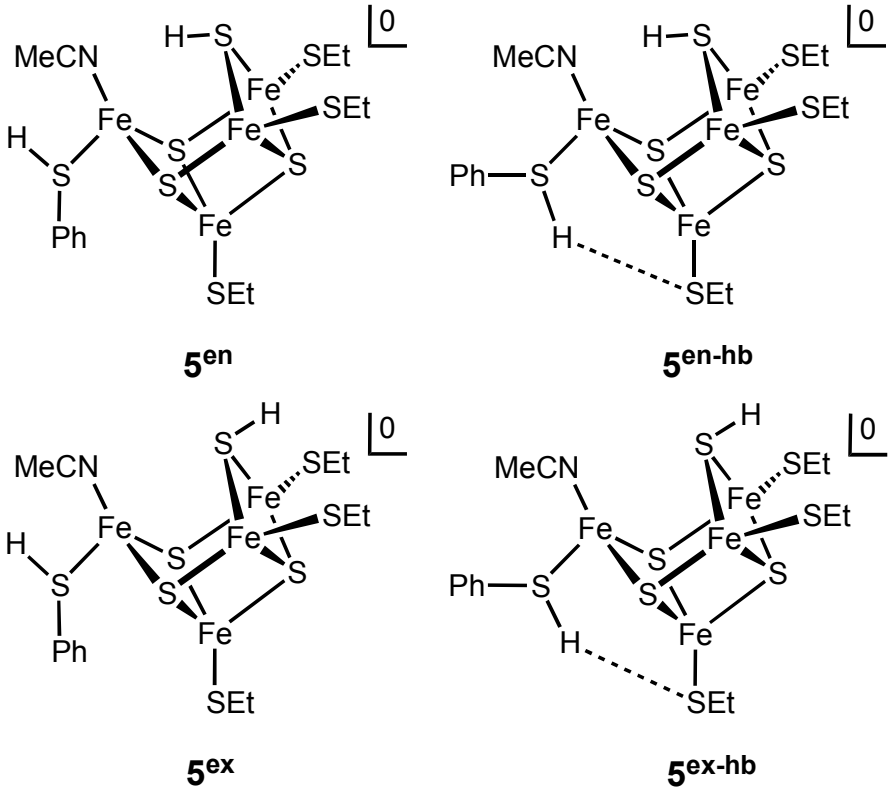

Scheme 3. The isomers of intermediate **5** for X = SEt. The broken line is a hydrogen bond.

Ligation by uncharged PhSH is unusual in coordination chemistry, but the favourable binding of PhSH occurs here because the Fe atom is under-coordinated in the precursor intermediate. The calculated Fe-S distances for coordinated PhSH range 2.52 - 2.60Å for **Cl-4**^{ex}, **Cl-4**^{en} and the four isomers of intermediate **5**. This Fe-S(H)Ph distance range is ca 0.25Å longer than Fe-SPh = 2.33Å in $[Fe_4S_4(SPh)_4]^{2-}$.

Final stages of the mechanisms

The final stages (**5** → **P** in Fig. 3, **Cl-4** → **P** in Fig. 5) involve two deprotonations (of PhSH and μ-SH) and dissociation of MeCN. These need not occur in the order drawn for the two mechanisms, but it is reasonable to assume that dissociation of MeCN would be more favourable energetically after PhSH has been deprotonated to form PhS^- which is a stronger ligand at the unique Fe atom, and deprotonation of μ-SH would be expected to be more favourable energetically when there is three-coordination at the unique Fe atom where the Fe-(μ_3-S) bond is reformed. Therefore we would expect that the sequence of stages is as drawn: deprotonation of PhSH, then dissociation of MeCN, then deprotonation of μ-SH.

We have not attempted to simulate the deprotonation steps because our computational model is too simplified. For the dissociation of MeCN after PhSH has been deprotonated (step **6** → **7** in Fig. 3, **Cl-5** → **Cl-6** in Fig. 5) the calculated potential energy changes are small, ranging from -2 to +5 kcal mol^{-1} for X = Cl and SEt, depending on the conformations of PhS and the inclusion of COSMO energies. Various calculations show no indication that any of these final steps would have barriers inconsistent with our proposal that these last three steps are relatively fast.

Summary and Discussion

We provide here a revised mechanism for the acid-catalysed ligand substitution reactions of clusters $[Fe_4S_4X_4]^{2-}$, for the cases where X = Cl, Br, SEt, SBu^t or OPh, and the attacking nucleophile is PhSH, yielding $[Fe_4S_4X_3(SPh)]^{2-}$ as product. The essential tenets of the mechanism are as follows. (1) Protonation of μ_3-S of $[Fe_4S_4X_4]^{2-}$ causes the *severance of an Fe-S(H) bond and creates a unique three-coordinate Fe atom, primed for attack by nucleophiles.* (2) Substitution of X by PhS^- occurs at this unique Fe site and occurs by an indirect pathway involving initial displacement of X by acetonitrile, followed by displacement of coordinated acetonitrile by PhSH. (3) In the first part of the substitution process, X dissociates from the unique Fe atom in protonated form XH if X is SEt, SBu^t or OPh, or as X^- if Cl or Br. (4) The preprotonated ligands HSEt, $HSBu^t$ or HOPh dissociate relatively slowly, while Cl^- or Br^- dissociate rapidly. (5) In the second part of the substitution process, the dissociation of X or XH recreates three-coordination at the unique Fe atom, which is then attacked by PhSH. (6) When X = Cl or Br the rate of attack by PhSH is slower than the dissociation of X^-, and is the rate-determining step; in contrast, when X = SEt, SBu^t or OPh the rate of dissociation of XH is the rate-determining step, being slower than attack by PhSH.

This mechanistic framework is consistent with all kinetic data. Furthermore, kinetic features, such as the slow rates of protonation of the clusters, the absence of a kinetic primary isotope effect in the reactions with deuterated acids, and the insensitivity of the apparent pK_as of the protonated clusters to their compositions, which were difficult to reconcile with the earlier proposed mechanisms (Fig. 2), are a natural consequence of the change in the cluster core structure after protonation, which is the central supposition of the revised mechanism shown in Figs. 3 and 5.

The mechanism is supported by DF calculations of the structures of all intermediates, and DF simulations of some of the reaction steps. The dissociation of EtSH and association of PhSH are 'mirrored' processes, both involving three-coordinate Fe; the calculated barrier for dissociation, creating three-coordinate Fe is calculated to be about the same (ca 8 kcal mol^{-1}) as the exergonicity of the association of PhSH, relieving the three-coordination of Fe. This relationship is required in the mechanism for the X = SEt, SBu^t or OPh reactions, in which dissociation is slow relative to association. Maintenance of protonated sulfide (μ-SH) throughout the sequence is also essential in reducing the coordination of the unique Fe atom. Should μ-SH deprotonate at some stage the favourable pathway would be interrupted, and reprotonation would be needed to allow the acid-catalysed path to product.

There is little difference in the inherent stabilities of the *exo* and *endo* isomers of μ-SH throughout the mechanism. *Endo* μ-SH can be involved in additional hydrogen bonding in some of the intermediates, but this hydrogen bonding does not appear, from the DF calculations, to provide energetically significant stabilisation or to lower reaction barriers. It is probable that the

protonation and deprotonation steps involving Et_3NH^+ or Et_3N encounter steric interference when the *endo* isomer is involved.

The essential new feature – severance of an Fe-S(H) bond and creation of a three-coordinate (approximately planar) Fe atom in $[Fe_4S_3(SH)X_4]^-$ – is expected to be general, and the mechanistic consequences described here are expected to be generally applicable to other clusters containing μ_3-S including both natural clusters, such as $[Fe_4S_4(S\text{-cysteine})_4]$ occurring in many metalloenzymes, and synthetic cubanoid $\{MFe_3S_4\}^{n+}$ (M = Mo, W, Nb, Ta, Re and V) clusters. This conversion of triply-bridging S to doubly-bridging SH on protonation, and the absence of a stable triply-bridging SH group in these $\{Fe_4S_4\}$ clusters is corroborated by the absence of an unambiguous μ_3-SH group in the structures contained in the Cambridge Structural Database (June 2013), an absence noted also by Hidai and Kuwata in their review of SH ligands in metal complexes.[44] Our mechanism also involves RSH and PhOH ligands in intermediates: these protonated forms of common RS^- and RO^- ligands also are rare in coordination chemistry.[45-47,43]

Finally, it has been known for many years that addition of strong acids (such as HCl) to both natural and synthetic Fe-S-based clusters leads to destruction of the cluster.[48] It is tempting to suggest that the single protonation and associated Fe-S bond cleavage reaction described herein corresponds to the initial steps in such destructive reactions of clusters with stronger acids. A key feature of the methodology used for the reactions described herein is the use of relatively weak acids (such as $NHEt_3^+$) so that the protonation is controlled and limited. Limiting the protonation state of Fe-S-based clusters in this way, so that the cluster core remains intact but with a changed structure, could prove to be a useful strategy for the synthesis of new clusters.

Acknowledgements

This research is supported by the University of New South Wales, and was undertaken with the assistance of resources provided at the National Computational Facility at the Australian National University through the National Computational Merit Allocation Scheme supported by the Australian Government.

Table of contents graphic

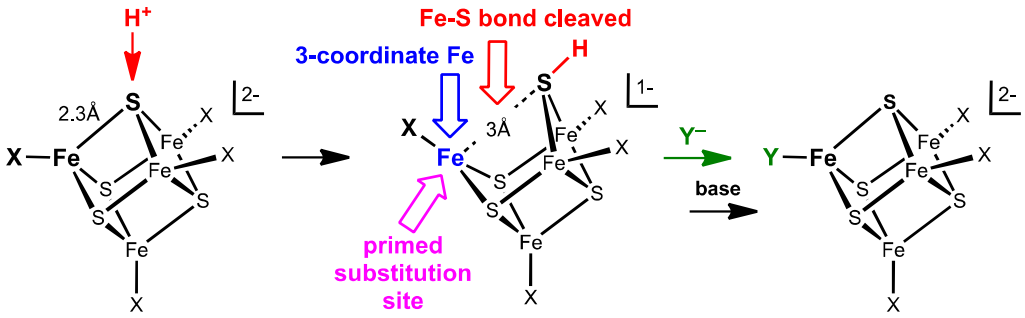

Table of contents sentence

Recognition that protonation of μ_3-S in $[Fe_4S_4X_4]^{2-}$ clusters causes breaking of an S-Fe bond provides a kinetically consistent general mechanism for the acid-catalysed substitution reactions of $[Fe_4S_4X_4]^{2-}$ clusters.

References

1 R. H. Holm, P. Kennepohl and E. I. Solomon, *Chem. Rev.*, 1996, **96**, 2239-2314.

2 H. Beinert, M. C. Kennedy and C. D. Stout, *Chemical Reviews*, 1996, **96**, 2335-2374.

3 H. Beinert, R. H. Holm and E. Munck, *Science*, 1997, **277**, 653-659.

4 D. C. Rees, *Annu. Rev. Biochem.*, 2002, **71**, 221-246.

5 S. C. Lee and R. H. Holm, *Chem. Rev.*, 2004, **104**, 1135-1157.

6 D. C. Rees, F. A. Tezcan, C. A. Haynes, M. Y. Walton, S. Andrade, O. Einsle and J. A. Howard, *Phil. Trans. Roy. Soc. A*, 2005, **363**, 971-984.

7 M. Can, F. A. Armstrong and S. W. Ragsdale, *Chemical Reviews*, 2014, **114**, 4149-4174.

8 I. Dance, *Inorg Chem*, 2013, **52**, 13068-13077.

9 A. Alwaaly, I. Dance and R. A. Henderson, *Chemical Communications*, 2014, **50**, 4799-4802.

10 R. A. Henderson, *Coord. Chem. Rev.*, 2005, **249**, 1841-1856.

11 R. A. Henderson, *Chem. Rev.*, 2005, **105**, 2365-2437.

12 W. P. Jencks, *Chemical Society Reviews*, 1981, **10**, 345-375.

13 T. J. Przystas, J. R. Ward and A. Haim, *Inorganic Chemistry*, 1973, **12**, 743-749.

14 G. R. Dukes and R. H. Holm, *J.Am.Chem.Soc.*, 1975, **97**, 528-533.

15 R. A. Henderson and K. E. Oglieve, *J. Chem. Soc., Dalton Trans.*, 1993, 1467-1472.

16 R. A. Henderson and K. E. Oglieve, *Journal of the Chemical Society, Dalton Transactions*, 1993, 1473-1476.

17 R. A. Henderson and K. E. Oglieve, *Journal of the Chemical Society, Chemical Communications*, 1994, 377-379.

18 B. Delley, *J. Chem. Phys.*, 1990, **92**, 508-517.

19 B. Delley, in *Modern density functional theory: a tool for chemistry*, eds. J. M. Seminario and P. Politzer, Elsevier, Amsterdam, 1995, p. 221-254

20 B. Delley, *J. Chem. Phys.*, 2000, **113**, 7756-7764.

21 I. G. Dance, in *Transition Metal Sulfur Chemistry: Biological and Industrial Significance*, eds. E. I. Stiefel and K. Matsumoto, American Chemical Society, Washington, DC, USA, 1996, p. 135-152

22 I. Dance, *J. Chem. Soc., Chem. Commun.*, 1998, 523-530.

23 I. Dance, *J. Am. Chem. Soc.*, 2005, **127**, 10925-10942.

24 I. Dance, *Dalton Trans.*, 2011, **40**, 6480-6489.

25 K. Izutsu, 'Acid-Base Dissociation Constants in Dipolar Aprotic Solvents', Blackwell Scientific, Oxford, UK, 1990.

26 B. Garrett and R. A. Henderson, *Dalton Trans*, 2005, 2395-2402.

27 B. G. Cox, 'Acids and Bases Solvent Effects on Acid-Base Strength', Oxford University Press, Oxford, UK., 2013.

28 The full rate law for the mechanism in Figure 3 is shown in Equation (2'). This rate law is derived assuming that the two initial protonation steps (K_0'and K_0) and the binding of MeCN (K_D) are rapidly established equilibria, and dissociation of X^- (k_e) is rate-limiting.

$$\text{Rate} = \frac{K_0'K_0K_D'k_e[Fe_4S_4X_4^{2-}][NHEt_3^+]^2/[NEt_3]^2}{1 + K_0'[NHEt_3^+]/[NEt_3](1 + K_0[NHEt_3^+]/[NEt_3])} \qquad (2')$$

If K_0' $[NHEt_3^+]/[NEt_3] > 1$ (i.e. the K_0' equilibrium lies to the right hand side), and Equation (2') simplifies to Equation (2).}

29 The experimental rate law for the acid-catalysed substitution exhibits a first order dependence on the concentration of PhSH. Whilst this dependence on the concentration of PhSH could be consistent with a mechanism involving direct attack of PhSH at **Cl-1**, this is unlikely. There is no obvious reason why, when X = halide, attack of PhSH displaces X, but when X = EtS, Bu^{t}S or PhO, MeCN displaces X.

30 The full rate law for the mechanism in Figure 5 is shown in Equation (3'). This rate law is derived assuming that the two protonation steps (K_0), the binding of MeCN (K_D) and dissociation of X^- (K_e) are rapidly established equilibria, and binding of PhSH (k_f) is rate-limiting.

$$\text{Rate} = \frac{K_0K_D'K_e'k_f[Fe_4S_4X_4^{2-}][PhSH][NHEt_3^+]/[NEt_3]}{1 + K_0[NHEt_3^+]/[NEt_3](1 + K_D' + K_D'K_e')} \qquad (3')$$

Under the experimental conditions the concentration of Cl^- is small and constant ($[Cl^-]$ = $0.25[Fe_4S_4Cl_4^{2-}] = 2.5 \times 10^{-5}$ dm^3 mol^{-1} s^{-1}). The interpretation of experiments where the concentration of Cl^- is varied (by the addition of $[NEt_4]Cl$) is complicated because Cl^- binds to the cluster and perturbs the rate. Since $K_0(1 + K_D' + K_D'K_e')$ is a constants, Equation (3′) is of the same form as observed experimentally.[17] If K_D' and $K_D'K_e'$ are small compared to 1, then Equation (3′) simplifies to Equation (3).}

[31] A. Klamt and G. Schüürmann, *J. Chem.Soc., Perkin Trans. 2*, 1993, 799-805.

[32] J. Andzelm, C. Kolmel and A. Klamt, *J. Chem. Phys.*, 1995, **103**, 9312-9320.

[33] B. Delley, *Molecular Simulation*, 2006, **32**, 117-123.

[34] I. Dance, *Molecular Simulation*, 2008, **34**, 923-929.

[35] I. Dance, *Molecular Simulation*, 2011, **37**, 257.

[36] J. Thar, W. Reckien and B. Kirchner, *Topics in Current Chemistry*, 2007, **268**, 133-171.

[37] R. A. Henderson and K. E. Oglieve, *Journal of the Chemical Society, Dalton Transactions*, 1999, 3927-3934.

[38] F. Wilkinson, A. F. Olea, D. J. McGarvey and D. R. Worrall, *J. Braz. Chem. Soc.*, 1995, **6**, 211-220.

[39] J. Bell, A. J. Dunford, E. Hollis and R. A. Henderson, *Angewandte Chemie International Edition*, 2003, **42**, 1149-1152.

[40] B. Garrett and R. A. Henderson, *Dalton Transactions*, 2010, **39**, 4586-4592.

[41] K. Bates and R. A. Henderson, *Inorg. Chem.*, 2008, **47**, 5850-5858.

[42] K. Bates, B. Garrett and R. A. Henderson, *Inorg. Chem.*, 2007, **46**, 11145-11155.

[43] E. S. F. Ma, S. J. Rettig, B. O. Patrick and B. R. James, *Inorganic Chemistry*, 2012, **51**, 5427-5434.

[44] S. Kuwata and M. Hidai, *Coord. Chem. Rev.*, 2001, **213**, 211-305.

[45] S. A. Wander, J. H. Reibenspies, J. S. Kim and M. Y. Darensbourg, *Inorganic Chemistry*, 1994, **33**, 1421-1426.

[46] C. B. Allan, G. Davidson, S. B. Choudhury, Z. Gu, K. Bose, R. O. Day and M. J. Maroney, *Inorganic Chemistry*, 1998, **37**, 4166-4167.

[47] R. Zaffaroni, T. B. Rauchfuss, D. L. Gray, L. De Gioia and G. Zampella, *Journal of the American Chemical Society*, 2012, **134**, 19260-19269.

[48] W. H. Orme-Johnson, *Annual Review of Biochemistry*, 1973, **42**, 159-204.